Parametric-Combustion Modeling of Crude Oil-Spilled Mangrove Vegetation

Agberegha, Orobome Larry
Department of Mechanical Engineering
Federal university of Petroleum Resources, Effurun, Nigeria

Nwigbo, Chuka Solomon
Department of Mechanical Engineering
Nnamdi Azikiwe University, Awka

Godspower Edafeadhe
Department of Mechanical Engineering
Delta State Polytechnics, Otefe-Ohara

Abstract

Combustion, or burning, has been defined as a high-temperature exothermic redox chemical reaction between a fuel (the reductant) and an oxidant, usually atmospheric oxygen, that produces oxidized, often gaseous products, in a mixture termed as smoke. The modeling of turbulent combustion is complex and requires the consideration of different physico-chemical processes involving a vast range of time and length scales as well as a large number of scalar quantities. In modeling combustion, the fuel was considered as single gas species, the air and products referred to as "lumped species". By implication, therefore the fuel for the combustion was considered a lumped species representing a mixture of gas species that transport together (i.e., the lumped species has a single set of transport properties); the lumbed species was assumed to react together. From our modeling simplication, the lumped species was treated as a single species; consequently, to reduce the number of transport equations from solving explicitly seven transport equations to the lowest possible number of equations we assume a single-step reaction. it is observed that irrespective of the computational frame number as well as the computational timestep, the maximum temperature field is 1000^{o}C and the maximum heat release rate per unit area is 150 kW/m^2.

Keywords: Fire Dynamics Simulator (FDS), Combustion Modeling, finite rate Chemistry Model (FRC)

I. INTRODUCTION

The goal of every modeling study is to simplify complex physics problems to simple physics ones; in a sense, the act of this simplification is making informed assumptions. In their FDS user manual, McGrattan et. al. (2013) gave guidelines in solving these problems, thus: in order to make progress, the questions that are asked have to be greatly simplified. To begin with, instead of seeking a methodology that can be applied to all fire problems, we begin by looking at a few scenarios that seem to be most amenable to analysis. Hopefully, the methods developed to study these "simple" problems can be generalized over time so that more complex scenarios can be analyzed. Second, we must learn to live with idealized descriptions of fires and approximate solutions to our idealized equations. Finally, the methods should be capable of systematic improvement. As our physical insight and computing power grow more powerful, the methods of analysis can grow with them.

However, Carlsson (1999) admonishes the modelers to recognize the fundamental features as well as the limitations of his or her computational tools. Carlsson (1999 went further: The models, whether they are programmed as part of a computer code or not, are not reality but merely a description, usually a simplification, of a real process or phenomenon. Nevertheless, once the difference between reality and the models has been understood and accepted the user should feel free to play the game of modelling.

True to their words, the science of modeling fire as with every natural phenomenon or processes has so developed. Predicting these phenomena is challenging, and experimental data are required to validate the code's accuracy. Clearly, intermediate and large-scale tests are required; however they are expensive and time consuming. LInteris et al. 2004

In predicting this challenging phenomenon, McGrattan et al. 2013, suggested that the difficulties revolve about three issues: First, there are an enormous number of possible fire scenarios to consider due to their accidental nature. Second, the physical insight and computing power required to perform all the necessary calculations for most fire scenarios are limited. Any fundamentally based study of fires must consider at least some aspects of bluff body aerodynamics, multi-phase flow, turbulent mixing and combustion, radiative transport, and conjugate heat transfer; all of which are active research areas in their own right. Finally, the "fuel" in most fires was never intended as such. Thus, the mathematical models and the data needed to characterize the degradation of the condensed phase materials that supply the fuel may not be available.

This work seeks to model combustion of compartment fire so as to understand how combustion proceeds and how it spreads in the computational-combustion space. Lump specie approach was used in the combustion modeling as the mangrove as well as the spilled crude oil was modeled as a lumpsome, i. e. as a lump specie.

Fire Dynamics Simulator (FDS) is a computational fluid dynamics (CFD) model of fire-driven fluid flow. The computer program solves numerically a large eddy simulation form of the Navier–Stokes equations appropriate for low-speed, thermally-driven flow,

with an emphasis on smoke and heat transport from fires, to describe the evolution of fire. Wikipeadia, 2018. The limitation of this model is averaging procedure at the root of the model equations.

The FDS algorithm is made of (FDS user manual): Low Mach, large-eddy simulation (LES); Explicit, second-order, kinetic-energy-conserving numerics ; Structured, uniform, staggered grid; Simple immersed boundary method for treatment of flow obstructions; Generalized "lumped species" method (simplified chemistry using a reaction progress variable); Deardorff eddy viscosity subgrid closure; Constant turbulent Schmidt and Prandtl numbers; Eddy dissipation concept (fast chemistry) for single-step reaction between fuel and oxidizer; Gray gas radiation with finite volume solution to the radiation transport equation

II. COMBUSTION MODELING

Combustion, or burning, is a high-temperature exothermic redox chemical reaction between a fuel (the reductant) and an oxidant, usually atmospheric oxygen, that produces oxidized, often gaseous products, in a mixture termed as smoke. (Wikipedea, 2018). Combustion in practice is usually very complex, with a large number of strongly interactive sub-processes involved, including chemical reactions, turbulent flow and radiative heat transfer Yan, (1999).

The combustion phenomena can be subdivided into a large set of interconnected phenomena like flow, turbulence, thermodynamics, chemical kinetics, radiation, extinction, ignition etc Magnussen, (2015).

The modeling of turbulent combustion is complex and requires the consideration of different physico-chemical processes involving a vast range of time and length scales as well as a large number of scalar quantities. Consequently, requirements for computational resources to perform detailed simulations that `directly' capture the oxidation of realistic fuels remains intractable in practical applications. To reduce the computational complexity, various combustion models are developed. Wu, (2017).
The following models of combustion

A. The Eddy Dissipation Concept

The Eddy Dissipation Concept of Magnussen is a general concept for treating the interaction between the turbulence and the chemistry in flames which offers the opportunity to treat the turbulence-chemical kinetic interaction in a stringent conceptual way at the same time as it takes care of many of the important characteristics of the turbulence. The EDC has been applied, without the need for changing constants, for a great variety of premixed and diffusion controlled combustion problems, both where the chemical kinetics is faster than the overall fine structure mixing as well as in cases where the chemical kinetics has a dominating influence. It is widely used for combustion modelling for a great variety of combustion environments with great success, and it is included in a number of commercially available computer codes, unfortunately, not always implemented in the conceptual best way. The is based on the philosophy of the non-homogeneous, localized, intermittent characteristics of the dissipation, it is a reactor concept including a fine structure reactor and its surrounding where reactions may take place both in the surroundings and in the fine structures. Key factors are: mass fraction contained in the fine structures, mass transfer rate between the fine structures and the surrounding fluids, reacting fraction of the fine structures. (Magnussen, 2015)

In his work, Numerical Modeling of Turbulent Combustion and Flame Spread, Yan (1999), in carrying out combustion modeling, modified the Eddy Dissipation concept of Magnussen. Part of his work is briefly presented: The ratio of turbulence kinetic energy and its dissipation rate, k/ε, indicates a dissipation time scale. By dimensional argument, we may estimate the dissipation rate of a general variable φ as $c_\varphi \frac{\bar{\varphi}_* \varepsilon}{k}$, where $\varphi_* = \varphi^{\dagger\dagger^2}$ and c_φ is an empirical proportion coefficient.

Based on these arguments, the mean combustion rate can be estimated as $c_\varphi \rho \frac{(\bar{\varphi}_*)^{0.5} \varepsilon}{k}$, with φ representing the mass fraction. The mean reaction rate is modeled by the dissipation rate of reactant and/or product eddies as

$$R_J = -\rho \frac{\varepsilon}{\kappa} \min\left(c_r \bar{Y}_J, c_r \frac{\bar{Y}_{ox}}{s}\right) \quad [1]$$

$$R_J = -\rho \frac{\varepsilon}{\kappa} \min\left(c_r \bar{Y}_J, c_r \frac{\bar{Y}_{ox}}{s}, c_p \frac{\bar{Y}_p}{1+s}\right) \quad [2]$$

Where the subscripts r,f ox and p in the above equation denotes reactants, fuel, oxidant and products, respectively.

B. A Finite Rate Chemistry Model (FRC)

The finite rate chemistry models, it has been proven, are better at handling flows that involve variable Lewis number mixing, extinction, ignition, emissions, fuel modulation, and combustion with multiple modes. Shi et al. (2017) . To avoid interpolation between grids and particles in Lagrangian formulation, Yang et. al. (2018) would employ an Eulerian formulation to track the detailed species transport. The Favre-filtered fully compressible Navier-Stokes equations of mass, momentum, energy, and species concentrations are given as follows Yang et. al. (2018):

$$\frac{\partial \bar{\rho}}{\partial t} + \frac{\partial \bar{\rho} \tilde{u}_i}{\partial x_i} = 0 \quad [3]$$

$$\frac{\partial \bar{\rho} \tilde{u}_i}{\partial t} + \frac{\partial \left(\bar{\rho} \tilde{u}_i \tilde{u}_j + \bar{p} \delta_{ij}\right)}{\partial x_j} = \frac{\partial (\tilde{\tau}_{ij} - \tau_{ij}^{sgs})}{\partial x_j} \quad [4]$$

$$\frac{\partial \bar{\rho} \tilde{E}}{\partial t} + \frac{\partial ((\bar{\rho} \tilde{E} + \bar{p}) \tilde{u}_i)}{\partial x_i} = \frac{\partial}{\partial x_i}\left(q_i + \tilde{u}_j \tilde{u}_{ij} - Q_i^{sgs} - H_i^{sgs} + \sigma_i^{sgs}\right) \quad [5]$$

$$\frac{\partial \bar{\rho} \tilde{Y}_k}{\partial t} + \frac{\partial (\bar{\rho} \tilde{u}_j \tilde{Y}_k)}{\partial x_j} = \frac{\partial}{\partial x_j}\left(\bar{\rho} \tilde{u}_{k,j} \tilde{Y}_k - \Phi_{\mathrm{k,j}}^{\mathrm{sgs}}\right) + \bar{\omega}_k \quad [6]$$

In Eq. [6], the pressure gradient term $\partial p\bar{\delta}ij/\partial xj$ is proportional to $1/M2$. In low Mach flows, this term becomes singular and creates great numerical challenges, which makes preconditioning scheme necessary for fully compressible solver.

C. *Flamelet/Progress Variable (FPV) Model*

In the FPV model Pierce and Moin, (2004); Huo and Yang, (2017), instead of filtered species equations, transport equations of filtered mixture fraction and filtered progress variable are tracked during the simulation:

$$\frac{\partial \bar{\rho}\tilde{Z}}{\partial t} + \frac{\partial (\bar{\rho}\tilde{u}_i\tilde{Z})}{\partial x_i} = \frac{\partial}{\partial x_i}\left(\bar{\rho}(\tilde{\alpha}_Z + \alpha_t)\frac{\partial \tilde{Z}}{\partial x_i}\right) \quad [7]$$

$$\frac{\partial \bar{\rho}\tilde{C}}{\partial t} + \frac{\partial (\bar{\rho}\tilde{u}_i\widetilde{C})}{\partial x_i} = \frac{\partial}{\partial x_i}\left(\bar{\rho}(\tilde{\alpha}_C + \alpha_t)\frac{\partial \tilde{C}}{\partial x_i}\right) + \bar{\dot{\omega}}_C \quad [8]$$

Without solving the species transport equation, FPV model assumes constant Lewis number for diffusivities $\tilde{\alpha}_Z$ and $\tilde{\alpha}$, thereby cannot capture differential diffusion effects. In the regions with low turbulence intensity, turbulent diffusivity α_t is smaller than $\tilde{\alpha}_Z$ and $\tilde{\alpha}_C$, and differential diffusion effects become important, leading to relatively larger errors. The source term $\bar{\dot{\omega}_C}$ for the filtered progress variable $\widetilde{C}$ can only be roughly estimated, and is integrated explicitly assuming the timescale of progress variable is larger than time step size Δt, which may not be true. Yang et. al. (2018)

D. *The Laminar Flamelet Model*

The steady laminar flamelet model pioneered by Peters,(2000) provides advantages of easy implementation and low computational cost, however, there are limitations. Firstly, the mixture fraction essentially does not carry any information about the chemical states. The model chooses the filtered dissipation rate of mixture fraction as an additional parameter to account for the flame stretching effect. However, it does not provide a unique mapping from mixture fraction to the corresponding reaction state. A pure mixing of fuel and oxidizer cannot be accounted by the steady laminar flamelet model if the local scalar dissipation rate is close to the quenching limit. Yang et.al. (2018). However, the steady laminar flamelet model, as it is with all computational combustion methods, is not without its fair share of inherent limitations. Gao et. al., (2016); Gao et. al. (2017a) and Gao et. al. (2017b) in their masterpiece at various conferences - *54th AIAA Aerospace Sciences Meeting, 55th AIAA Aerospace Sciences Meeting and 53rd AIAA/SAE/ASEE Joint Propulsion Conference* - between 2016 and 2017 established that the coexistence and interaction between auto-ignition kernels and flame sheet cannot be captured. To address these limitations of the steady laminar flamelet model, Huo and Yang, (2017) and Pierce and Moin, (2004) proposed the FPV model by incorporating a transport equation to track a progress variable. The FPV model, itself, was further developed by Pierce and Moin, (2004) to account for low-level of extinction, ignition, and unsteady mixing effect to some extent. Even with these modifications, it is instructive to note that two problems yet exist: one, it cannot handle multiple-feed streams unless adding a third parameter, which makes the look-up table very difficult to handle due to the large computer memory requirement and time to build up the table. Two, the higher-dimension look-up table results in a more complicated data retrieval process and coarser table grid, which could introduce higher interpolation errors. In using the flamelet model, the following assumptions are made (http://www.afs.enea.it/project/neptunius/docs/fluent/html/th/node156.htm): The following restrictions apply to all flamelet models:

1) Only a single mixture fraction can be modeled; two-mixture-fraction flamelet models are not allowed.
2) The mixture fraction is assumed to follow the -function PDF, and scalar dissipation fluctuations are ignored.
3) Empirically-based streams cannot be used with the flamelet model.

1) Strain Rate and Scalar Dissipation

A characteristic strain rate for a counterflow diffusion flamelet can be defined as $\boldsymbol{a_s = v/2d}$, where $\boldsymbol{v}$ is the relative speed of the fuel and oxidizer jets, and dis the distance between the jet nozzles.

Instead of using the strain rate to quantify the departure from equilibrium, it is expedient to use the scalar dissipation, denoted by $\boldsymbol{\chi}$. The scalar dissipation is defined as

$$\chi = 2D|\nabla f|^2 \quad [9]$$

where D is a representative diffusion coefficient.

Note that the scalar dissipation, $\boldsymbol{\chi}$, varies along the axis of the flamelet. For the counterflow geometry, the flamelet strain rate

$a_s$can be related to the scalar dissipation at the position where $\boldsymbol{f}$ is stoichiometric by

$$\chi_{st} = \frac{a_s \exp(-2|erfc^{-1}(2f_{st})|^2)}{\pi} \quad [10]$$

Where $\boldsymbol{a_s}$ is characteristic strain rate
f_{st} is stoichiometry mixture fraction
erfc^{-1} is inverse complementary error function

E. *Probability Density Function, PDF, Model*

A turbulent combustion model based on the probability density function (PDF) approach was applied to spray combustion computations under simulated diesel engine conditions. This approach accounts for the effects of turbulence and of random dynamics of evaporating droplets on the mean rate of chemistry. Durand et. al. 1999 developed joint PDF models for the gaseous mixture variables where evaporating droplets are viewed as point sources. DuranD et. al. 1999 also carried out the Monte Carlo

modeling of joint PDF equation for mixture species, which also implemented using the multidimensional computational computer code KIVA II. Evaporation is included into stochastic processes. Micromixing term itself is treated here within the modified coalescence-dispersion model (Curl, 1963). It was shown, by Durand et. al. 1999, that the PDF equation model is able to predict experimental data significantly better than the Eddy-Break-Up model.

In each finite-difference cell the PDF for turbulent mixture is considered to be composed of *N* statistical particles. The ensemble average probability corresponding to the variable $X_v(\hat{X}_v < X_v < \hat{X}_v + d\hat{X}_v)$ is defined as a ratio of enseinble averaged particle nx_v associated with value $\hat{X}_v$ to the number *N* of the particles *(N* is constant for each cell) Durand et. al. 1999

$$P(X_v)\Delta X_v = \frac{nx_v}{N} \quad [11]$$

Averaged and variance values of X_v are defined as

$$\bar{X}_v = \int_0^\infty X_v \, \mathrm{P}(X_v)\, dX_v = \sum_{i=1}^{class} X_{vi} \frac{\mathrm{n_i}}{\mathrm{N}} = \frac{1}{\mathrm{N}} X_{vi} \quad [12]$$

$$\bar{X}_v'^2 = \int_0^\infty {X_v}^2 \, \mathrm{P}(X_v)\, dX_v = \frac{1}{N}\sum_{i=1}^{N}(X_v - \bar{X}_v)_i^2 \quad [13]$$

Ensembles of statistical particles are modified at each time step as a result of the stochastic simulation of finite-difference schemes associated with PDF convection-diffusion transport computations and micromixing-vaporization-chemistry terms.
The unconditional PDF balance equation was modeled by (Kuznetsov and Sabel'nikov, 1990)

$$\left.\begin{aligned} &\frac{\partial}{\partial t}\left[\left(\left(\rho|Y_v = \hat{Y}_v\right)\right)P(\hat{Y}_v)\right] + \nabla\left[\left(\rho\vec{V}|Y_v = \hat{Y}_v\right)P(\hat{Y}_v)\right] = \left[\left(\rho\dot{\omega}_{lg}|Y_v = \hat{Y}_v\right)P(\hat{Y}_v)\right] \\ &-\frac{\partial}{\partial \hat{Y}_v}\left[\nabla\left(\rho D\nabla Y_v|Y_v = \hat{Y}_v\right)P(\hat{Y}_v)\right] - \frac{\partial}{\partial \hat{Y}_v}\left[P(\hat{Y}_v)\left(\rho\dot{\omega}_{lg}|Y_v = \hat{Y}_v\right)(1-\hat{Y}_v)\right] \\ &-\frac{\partial}{\partial \hat{Y}_v}\left[P(\hat{Y}_v)\left(\rho\dot{\omega}_{chem}|Y_v = \hat{Y}_v\right)\right] \end{aligned}\right\} \quad [14]$$

Stollinger and Heinz, (2008)

$$\frac{\partial(\rho)F_\theta}{\partial t} + \frac{\partial(\rho)\bar{u}_i F_\theta}{\partial x_i} = -\frac{\partial(\rho)\left(\bar{u}_i''|\theta F_\theta\right)}{\partial x_i} - \sum_{\alpha=1}^{N_s}\frac{\partial}{\partial\theta_\alpha}\left((\rho)\frac{D\phi_\alpha}{Dt}\middle|\theta F_0\right) \quad [15]$$

Here (ρ) is the ensemble averaged mass density. A Favre decomposition $u_i = \bar{u}_i + u_i''$ is used for velocities. Favre decompositions of other variables will be represented in the same way, this means $\bar{\boldsymbol{Q}}$ refers to the mass-density averaged mean of any variable Q, and the corresponding Favre fluctuation is $Q'' = Q - \bar{Q}$. The sum convention is used throughout this paper for repeated Roman subscripts but not for Greek subscripts. $(\bar{u}_i''|\theta)$ and $\left(\frac{D\bar{\phi}_\alpha}{Dt}\middle|\theta\right)$denote conditional Favre averages, where θ is the sample space scalar vector. According to the Navier-Stokes equations, the substantial derivatives $\frac{D\phi_\alpha}{Dt}$ of scalars are given by

$$\frac{\partial\phi_\alpha}{\partial t} = \frac{1}{\rho}\frac{\partial}{\partial x_k}\left(\frac{\rho\nu}{Sc_\alpha}\frac{\partial\phi_\alpha}{\partial x_k}\right) + S_\alpha \quad [16]$$

Here, ν denotes the kinematic viscosity, Sc_α is the Schmidt number of scalar α and
S_α is a source rate due to chemical reactions.
Further simplication yields the scalar PDF transport equation

$$\frac{\partial(\rho)F_\theta}{\partial t} + \frac{\partial(\rho)\bar{u}_i F_\theta}{\partial x_i} = \frac{\partial}{\partial x_k}(\rho)\left[\frac{\bar{\nu}}{Sc_\alpha}\frac{\partial F_\theta}{\partial x_k} - \left(\bar{u}_i''|\theta F_\theta\right)\right] - \sum_{\alpha=1}^{N_s}\frac{\partial}{\partial\theta_\alpha}(\rho)[M_\alpha'' + S_\alpha]F_\theta \quad [17]$$

III. GOVERNING EQUATIONS

The classical description of a combustion problem is based on continuum mechanics, assuming local mechanic and thermal equilibrium and local chemical homogeneity. Yan 1999.

The governing equations for such flames are the conservation equations of mass, momentum and energy of the gas mixture, the balance equations of mass for the species involved and the thermal and caloric equations of state Veynante, (2011), Williams (1985). These are presented in the next subsection.

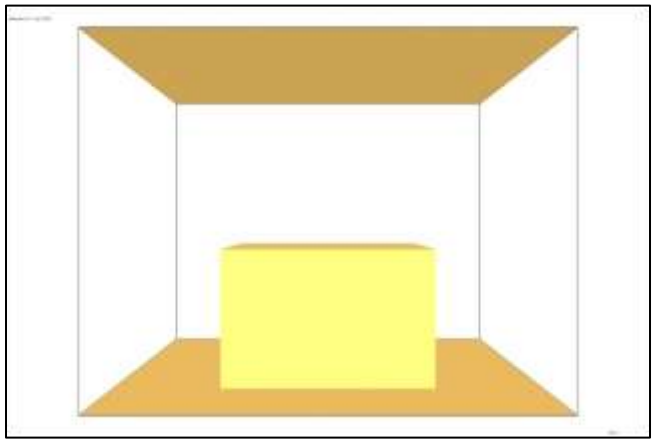

Fig. 1: Geometrically modeled computational domain

A. Large Eddy Simulation, LES, formalism:

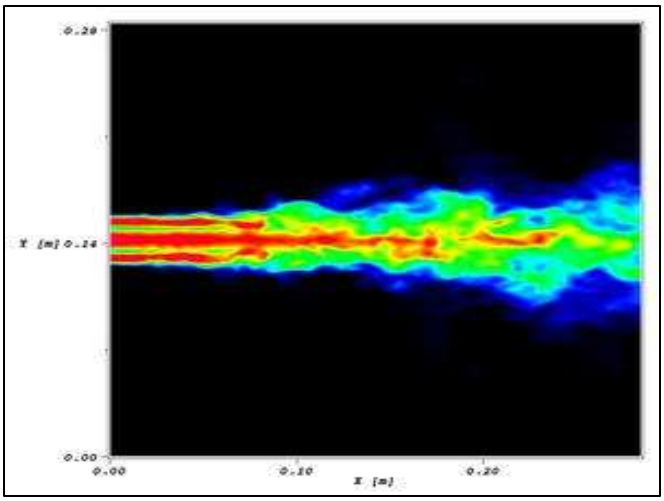

Fig. 2: Large eddy simulation of a turbulent gas velocity field.(Wikipedia, 2018)

Large eddy simulation (LES) is a mathematical model for turbulence used in computational fluid dynamics. Large eddy simulation is currently applied in a wide variety of engineering applications, including combustion, acoustics, and simulations of the atmospheric boundary layer.The simulation of turbulent flows by numerically solving the Navier–Stokes equations requires resolving a very wide range of time and length scales, all of which affect the flow field. The principal idea behind LES is to reduce the computational cost by ignoring the smallest length scales, which are the most computationally expensive to resolve, via low-pass filtering of the Navier–Stokes equations. Such a low-pass filtering, which can be viewed as a time- and spatial-averaging, effectively removes small-scale information from the numerical solution. This information is not irrelevant, however, and its effect on the flow field must be modeled, a task which is an active area of research for problems in which small-scales can play an important role, such as near-wall flows, reacting flows, and multiphase flows. (Wikipedia, 2018)

A large Eddy Simulation, LES, model explicitly calculates the large-eddy field and parameterizes the small eddies. The large eddies in the atmospheric boundary layer are believed to be much more important and more flow-dependent than the small eddies. The LES model results are therefore believed to be relatively insensitive to the parameterization of scheme for the small eddies. Moeng, (1984)

The equations for large-eddy simulation (LES) are derived by applying a low-pass filter, parameterized by a width D, to the transport equations for mass, momentum and energy(FDS user manual)

$$\tilde{\rho}(x,t) = \frac{1}{\Delta}\int_{x-\Delta/2}^{x+\Delta/2} \rho(r,t)dr. \qquad [18]$$

In FDS, the filter width D is equivalent to the local cell size dx and is a key parameter in the submodels for the turbulent viscosity and the reaction time scale discussed later. The practice of taking $\boldsymbol{\Delta} = \boldsymbol{\delta}$x is called implicit filtering.

Moeng, (1984) applied the Large Eddy Simulation, LES, to study Planetary Boundary-Layer Turbulence. Herein are some of the governing equations used:

The equation of motion for resolved-velocity components:

$$\frac{\partial \bar{u}}{\partial t} = \overline{\bar{v}\xi_z} - \overline{\bar{w}\xi_y} + f\bar{v} - \frac{\partial P^*}{\partial x} - \frac{\partial(\bar{\rho})}{\partial x} - \frac{\partial \tau_{xx}}{\partial x} - \frac{\partial \tau_{xy}}{\partial y} - \frac{\partial \tau_{xz}}{\partial z} \qquad [19]$$

$$\frac{\partial \bar{v}}{\partial t} = \overline{\bar{w}\xi_x} - \overline{\bar{w}\xi_z} + f\bar{u} - \frac{\partial P^*}{\partial y} - \frac{\partial(\bar{\rho})}{\partial y} - \frac{\partial \tau_{xy}}{\partial x} - \frac{\partial \tau_{yy}}{\partial y} - \frac{\partial \tau_{yz}}{\partial z} \qquad [20]$$

$$\frac{\partial \bar{w}}{\partial t} = \overline{\bar{u}\xi_y} - \overline{\bar{v}\xi_x} + \frac{g\bar{\theta}}{\theta_0} - \frac{\partial P^*}{\partial z} - \frac{\partial \tau_{xz}}{\partial x} - \frac{\partial \tau_{yz}}{\partial y} - \frac{\partial \tau_{zz}}{\partial z} - \left[\bar{u}\bar{\zeta}_y - \bar{u}\bar{\zeta}_x + \frac{g\bar{\theta}}{\theta_0} - \frac{\partial P^*}{\partial z} - \frac{\partial \tau_{xz}}{\partial x} - \frac{\partial \tau_{yz}}{\partial y} - \frac{\partial \tau_{zz}}{\partial z}\right] \qquad [21]$$

The continuity equation is thus

$$\frac{\partial \bar{u}}{\partial x} + \frac{\partial \bar{v}}{\partial y} + \frac{\partial \bar{w}}{\partial z} = 0 \qquad [22]$$

Using the poisson equation, the pressure filed may be resolved by taken the divergence of the of motion:

$$\nabla^2 P^* = \frac{\partial H_x}{\partial x} + \frac{\partial H_y}{\partial y} + \frac{\partial H_z}{\partial z} \qquad [23]$$

Where H_x, H_y and H_z are the sums of the Right-hand sides (except the $\boldsymbol{P}^*$ gradient terms)

B. Mass and Species Modeling

Mass and Species modeling may be described as a computational science where a group of physical bodies – real or abstracted - and a measure of its resistance to acceleration (or change in its state of motion) at the application of a net force is computationally studied.

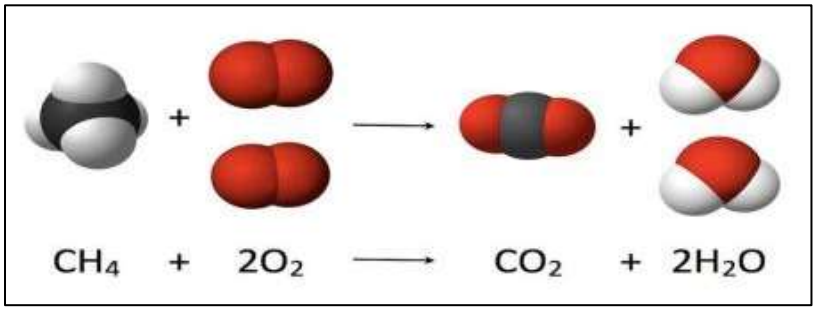

Fig. 3: Three dimensional methane combustion (Thoughtco, 2018)

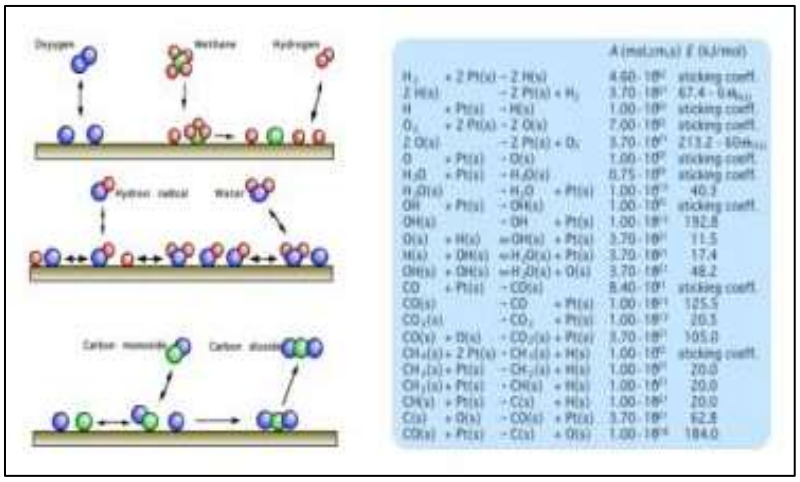

Fig. 4: schematic of the Surface reaction mechanism of methane oxidation (Westbrook,2004)

From the lumped species, the primitive species can be recovered (FDS user manual) thus:

$$\begin{bmatrix} 0.77 & 0.00 & 0.73 \\ 0.23 & 0.00 & 0.00 \\ 0.00 & 1.00 & 0.00 \\ 0.00 & 0.00 & 0.15 \\ 0.00 & 0.00 & 0.12 \end{bmatrix} \begin{bmatrix} \boldsymbol{Z_A} \\ \boldsymbol{Z_F} \\ \boldsymbol{Z_P} \end{bmatrix} = \begin{bmatrix} Y1 \\ Y2 \\ Y3 \\ Y4 \\ Y5 \end{bmatrix}$$

Where 1 is N_2, 2 is O_2, 3 is CH_4, 4 is CO_2 and 5 is H_20

In terms of primitive species, a one-step methane may be written as

$$CH_4 + 2O_2 + 7.52N_2 \rightarrow CO_2 + 2H_2O + 7.52N_2 \quad [24]$$

This is equivalent to (FDS user manual)

$$9.52\underbrace{0.21O_2 + 0.79N_2}_{Air,Z_0} + \underbrace{CH_4}_{Feul,Z_1} \rightarrow 10.52\underbrace{(0.095CO_2 + 0.19H_2O + 0.715N_2)}_{Product,Z_2} \quad [25]$$

Where 9.52 moles of Air react with 1 mole of fuel to produce 10.52 products. Notice that the primitive species have been grouped by volume fraction into lumped species and the lumped species stoichiometric coefficients are the sum of the primitive species coefficients from Eq. (25). Note that 9.52 _ 0.21 is only approximately equal to 2. In practice the atom balance requires machine precision. To alleviate this issue, FDS internally normalizes the lumped species volume fractions and makes any necessary adjustments to the specified lumped stoichiometric coefficients. The lumped species mass fractions are denoted Z_i, i = 0 ;1; ::::N_Z, where N_Z is the number of tracked species. The Background species, Z_0, is found from $Z_0 = 1 - \sum_{i=1}^{N_Z} Z_i$. In the case of Eq. (2.3), two transport equations are solved (FDS user manual).

In mass and species transport, density is estimated thus:

$$\frac{\rho^*_{ijk} - \rho^n_{ijk}}{\delta t} + \nabla.(\bar{\rho}^{FL}u)^*_{ijk} = 0 \quad [26]$$

$$\frac{\rho^{n+1}_{ijk} - \frac{1}{2}(\rho^n_{ijk} + \rho^*_{ijk})}{\frac{1}{2}\delta t} + \nabla.(\bar{\rho}^{FL}u)^*_{ijk} = 0 \quad [27]$$

The species conservation equations [2.4] and [2.5] are simplified, including turbulent diffusion thus

$$\frac{(\rho Z_\alpha)^*_{ijk}-(\rho Z_\alpha)^n_{ijk}}{\delta t}+\nabla.(\bar{\rho}^{FL}u)^n_{ijk}=\nabla.(\rho D_\alpha \nabla Z_\alpha)^n_{ijk} \quad [28]$$

C. *Transport Equation*

The convection–diffusion equation is a combination of the diffusion and convection (advection) equations, and describes physical phenomena where particles, energy, or other physical quantities are transferred inside a physical system due to two processes: diffusion and convection. Depending on context, the same equation can be called the advection–diusion equation, drift–diffusion equation,[1] or (generic) scalar transport equation. (Wikipedia, 2018)
The transport equation is a partial differential equation of form Remski, (2014)

$$u_t + cu_x = 0 \quad [29]$$

Here, u is a function of two variables $x\ and\ t$, and the subscripts denote partial derivatives. We shall assume that c is a fixed constant given an initial condition

$$u(x,0)=f(x) \quad [30]$$

The transport equation Durand et al. (1999)

$$\frac{\partial}{\partial t}(\rho Z_\alpha)+\nabla.(\rho Z_\alpha u)=\nabla.(\rho D_\alpha \nabla Z_\alpha)+\dot{m}'''_\alpha+\dot{m}'''_{b,\alpha} \quad [31]$$

Here $\dot{m}'''_\alpha=\sum_\alpha \dot{m}'''_{b,\alpha}$ is the production rate of species by evaporating droplets or particles. Summing these equations over all species yields the original mass conservation equation because $\sum Z_\alpha = 1$ and $\sum \dot{m}'''_\alpha = 0$ and$\sum \dot{m}'''_{b,\alpha} = \dot{m}'''_b$, by definition because it is assumed that $\sum \rho D_\alpha \nabla Z_\alpha = 0$.

D. *Low Mach number Approximation*

For low speed applications like fire, Rehm and Baum (1978) observed that the spatially and temporally resolved pressure, p, can be decomposed into a "background" pressure, p(z; t), plus a perturbation, ˜ p(x;y; z; t), with only the background pressure retained in the equation of state (ideal gas law):

$$\bar{P}=\rho TR\sum_\alpha \frac{Z_\alpha}{W_\alpha}=\frac{\rho RT}{W} \quad [32]$$

Note that Z is the spatial coordinate in the direction of gravity; thus, the stratification of the atmosphere s included in the background pressure. The perturbation, $\bar{P}$, drives the fluid motion.

E. *Momentum Transport*

Noting the vector identity $(u.\nabla)u=\frac{\nabla|u|^2}{2}-u\ X\ w$ and defining the stagnation energy per unit mass, $H=\frac{|u|^2}{2}+\frac{\tilde{p}}{\rho}$, the momentum equation can be written (FDS user manual)

$$\frac{\partial u}{\partial t}-u\ X\ w+\rho\nabla(1/\rho)=\frac{1}{\rho}[(\rho-\rho o)g+f_b\nabla.\tau] \quad [33]$$

The term, f_b, represents the drag force exerted by the subgrid-scale particles and droplets. The viscous stress, t, is closed via gradient diffusion with the turbulent viscosity obtained from the Deardorff eddy viscosity model [Deardorff,1980;Pope, 2000]. It is convenient to write Eq. (2.6) in the form:

$$\frac{\partial u}{\partial t}+F+\nabla H=0 \quad [34]$$

so that a Poisson equation for the pressure can be derived by taking its divergence:

$$\nabla^2 H=-\left[\frac{\partial}{\partial x}(\nabla.u)+\nabla.F\right] \quad [35]$$

Note the appearance of the time derivative of the divergence. This is an important feature of the time marching scheme. Note also that the right hand side of the Poisson equation retains a term that includes the perturbation pressure, ˜ p**∇** (1/ **ρ**). This term accounts for the baroclinic torque. It is included on the right hand side of the Poisson equation by using its value from the previous time step. This approximation allows us to solve a separable form of the Poisson equation, for which there are fast, direct solvers that are optimized for uniform grids.

F. *Radiation*

The thermal radiation was modeled thus (FDS user manual):

$$\dot{q}'''_r \equiv -\nabla.\dot{q}''_r(x)=\kappa(x)[U(x)-4\pi I_b];\ U(x)=\int_{4\pi} I(x,s')ds' \quad [36]$$

Where $\kappa(x)$ is the absorption coefficient, $I_b(x)$ is the source term, and I (x, s) is the solution of the radiation transport equation for a non-scattering gray gas:

$$s.\nabla I(x,s)=k(x)[I_b(x)-I(x,s)] \quad [37]$$

G. *The Equation of State*

$$\bar{p_0}(z)=\ p_\infty \exp(-\int_{z_\infty}^{z}\frac{W_g}{RT_0(z')}dz') \quad [38]$$

where the subscript infinity generally refers to the ground. A linear temperature stratification of the atmosphere may be specified by the user such that $T_0(z) = T_\infty + \Gamma_z$ where T_∞ is the temperature at the ground and Γ is the lapse rate (e.g., $\Gamma = -0.0098\ K/m$ is the adiabatic lapse rate). Equation [37] may be simplified further:

$$\bar{p_0}(z) = p_\infty \left(\frac{T_0(z)}{T_\infty}\right)^{W_g/RT} \quad [39]$$

H. The Heterogeneous Multiscale Method, HMM

Though basically a review, Echekki and Mastorakos, (2011) applied The Heterogeneous Multiscale Methods to Combustion. The HMM algorithm, at each macro step is thus:

1) Given the current state of the macro variables U_n, reinitialize the micro-variables:
$$u_{n,0} = RU_n \quad [40]$$
2) Evolve the micro variables for some micro time steps:
$$u_{n,m+1} = \zeta_{\delta t}(u_{n,m}; U_n), m = 0, \dots, M-1; \quad [41]$$
3) Estimate D:
$$D_n = \wp_M(u_{n,0}, \dots, u_{n,M}); \quad [42]$$
4) Evolve the macro-variables for one macro time step using the macro-solver:
$$u_{n+1} = S_{\Delta t}(U_n; D_n) \quad [43]$$

Where *R* is some reconstruction operator that reinitializes the micro model in a way that is consistent with the current state of the macro variables, $\boldsymbol{\zeta_{\delta t}}t$ is the micro solver, which also depends on *Un* through the constraints, as indicated. $\wp_{\boldsymbol{M}}$ is some data processing operator which in general involves spatial/temporal/ensemble averaging.
This is sometimes referred to as the data estimator. Finally $\boldsymbol{S_{\Delta t}}$ is the macro solver.

I. Conservation Equations

1) Continuity Equation
$$\frac{\partial \rho}{\partial t} + \nabla.\rho u = 0 \quad [42]$$

2) Momentum Equation
$$\rho \frac{Du}{Dt} = \rho \frac{\partial u}{\partial t} + \rho u.\nabla u = -\nabla\rho + \nabla.\tau + \rho \sum_{k=1}^{N} Y_k f_k \quad [43]$$

3) Species Continuity ($k = 1, \dots, N$)
$$\rho \frac{DY_k}{Dt} = \rho \frac{\partial Y_k}{\partial t} + \rho u.\nabla Y_k = \nabla.(-\rho V_k Y_k) + \omega_k, \quad [44]$$

4) Energy Equation
$$\rho \frac{De}{Dt} = \rho \frac{\partial e}{\partial t} + \rho u.\nabla e = -\nabla.q - p\nabla.u + \tau:\nabla u + \rho \sum_{k=1}^{N} Y_k f_k.V_k \quad [45]$$

The nomenclature for equations [2.16] to [2.18] : $\boldsymbol{\rho}$ is mass density; u is velocity vector; *p* is pressure; f_k is body force associated with *k*th species per unit mass; $\boldsymbol{\tau}$ is viscous stress tensor; V*k* is diffusive velocity of the *k*th species, where the velocity of the *k*th species may be expressed as the sum of the mass-weighted velocity and the diffusive velocity, u+V*k*; $\boldsymbol{\omega_k}$ is *k*th species production rate; *e* is mixture internal energy, which may be expressed as $\boldsymbol{e = \sum_{k=1}^{N} h_k Y_k - p/\rho}$; q is heat flux, representing heat transfer by conduction, radiation and transport through species gradients and the Soret effect. Rajika and Narayana, (2016).

5) EULER'S Equations

Derived from the conservation laws of mass, momentum and energy, the Euler's equation is the fundamental/basic governing equations in fluid dynamics are the Euler's equation is the fundamental governing equation s in fluid dynamics. In deriving the Euler's equations or in its application, it characterize flows with no viscosity. The partial differential equation describing the Euler's equation are:

$$\frac{\partial \rho}{\partial t} + \frac{\partial \rho u_i}{\partial x_i} = 0 \quad [46]$$
$$\frac{\partial}{\partial t}\rho u_j + \frac{\partial}{\partial x_i}\rho u_i u_j + \frac{\partial p}{\partial x_i} = 0 \quad [47]$$
$$\frac{\partial \rho e}{\partial t} + \frac{\partial}{\partial x_i}(\rho u_i e) = 0 \quad [48]$$

The above equations are written using Einstein notation, in which matched pairs of indices refers to a summation Xu, (2014).

6) The Navier Stokes Equation

The Navier-Stokes equation is an equation derived from the Newton's second law of motion applied to a small moving blob of a viscous fluid. The Navier-Stokes equation is a generalization of Euler's equation. In its must explicit for, in three dimension, the Navier-Stokes equation Rajput, (2013)

$$B_x - \frac{1}{\rho}.\frac{\partial \rho}{\partial x} = \frac{du}{dt} - \nu\left[\frac{\partial^2 u}{\partial x^2} + \frac{\partial^2 u}{\partial y^2} + \frac{\partial^2 u}{\partial z^2}\right] \quad [49]$$
$$B_y - \frac{1}{\rho}.\frac{\partial \rho}{\partial y} = \frac{dv}{dt} - \nu\left[\frac{\partial^2 v}{\partial x^2} + \frac{\partial^2 v}{\partial y^2} + \frac{\partial^2 v}{\partial z^2}\right] \quad [50]$$
$$B_z - \frac{1}{\rho}.\frac{\partial \rho}{\partial z} = \frac{dv}{dt} - \nu\left[\frac{\partial^2 w}{\partial x^2} + \frac{\partial^2 w}{\partial y^2} + \frac{\partial^2 w}{\partial z^2}\right] \quad [51]$$

IV. MOMENTUM TRANSPORT AND PRESSURE

The solutions to the momentum transport and pressure models are:

A. Large Eddy Simulation (LES)

Then for any continuous field, f, a filtered field is defined as

$$\phi\ (x,y,z,t) \equiv \frac{1}{V_c}\int_{x-\delta x/2}^{x+\delta x/2}\int_{y+\delta y/2}^{y+\delta y/2}\int_{z-\delta z/2}^{z+\delta z/2}\phi(x',y',z',t)dx'dy'dz' \quad [52]$$

) The DNS Momentum Equation

The DNS momentum equation for the ith component of velocity is

$$\frac{\partial \rho u_i}{\partial t}+\frac{\partial}{\partial x_j}\left(\rho u_i u_j\right)=-\frac{\partial p}{\partial x_i}-\frac{\partial \tau_{ij}}{\partial x_j}+\rho g_i+f_{d,i}+\dot{m}_b'''u_{b,i} \quad [53]$$

In the two-phase modeling, the sixth term represents the drag force due to unresolved lagrangian particles. The bulk source term, $\dot{\boldsymbol{m}}_{\boldsymbol{b}}'''\boldsymbol{u}_{\boldsymbol{b},\boldsymbol{i}}$, accounts for the effects of pyrolysis or evaporation.

V. BOUNDARY CONDITIONS FORMULATION

The boundary condition for the computational space was modeled, with one face as open while all others are solid boundaries. For the solid boundary,

$$k\frac{T_g-T_w}{\delta n/2}=h\left(T_g-T_w\right) \quad [54]$$

In an open boundary condition, the temperature and species mass fractions take on their respective exterior values if the flow is incoming, and take on their respective values in the grid cell adjacent to the boundary if the flow is outgoing.

VI. RESULTS & DISCUSSIONS

Figure 5 to 25 show full rendering and simulations describing combustion, temperature, heat flux and radiative heat characterisations from frame 1.0, time step 1.8 to frame 190, to time step 342.

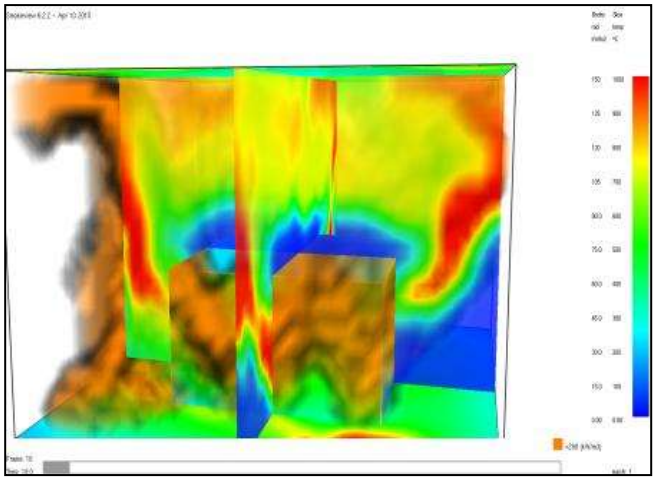

Fig. 5: simulation at frame 10, timestep 18

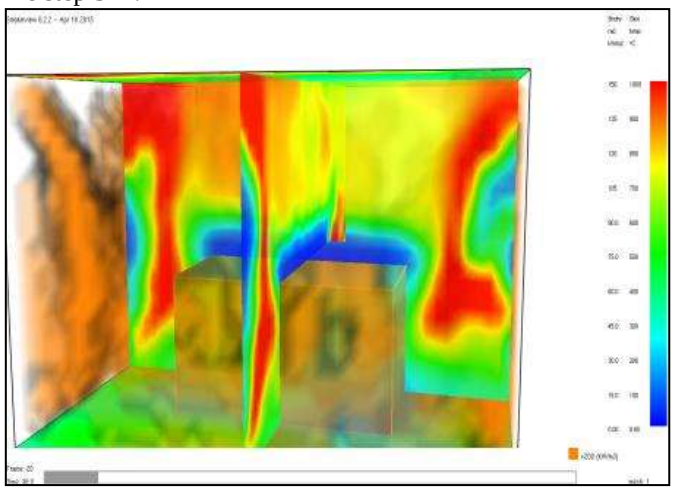

Fig. 6: simulation at frame 20, timestep 36

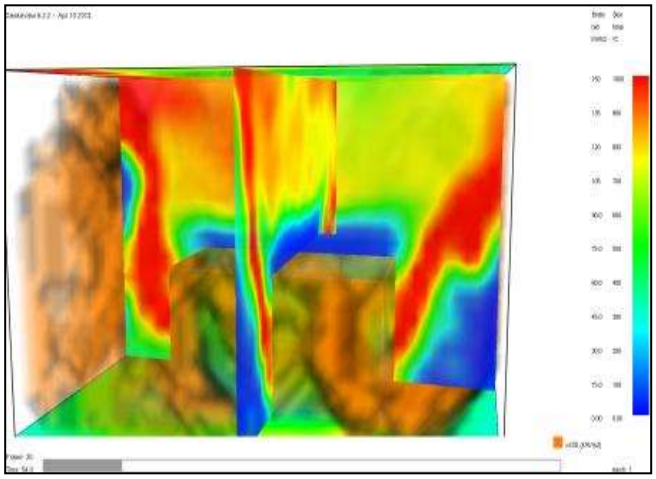

Fig. 7: simulation at frame 30, timestep 54

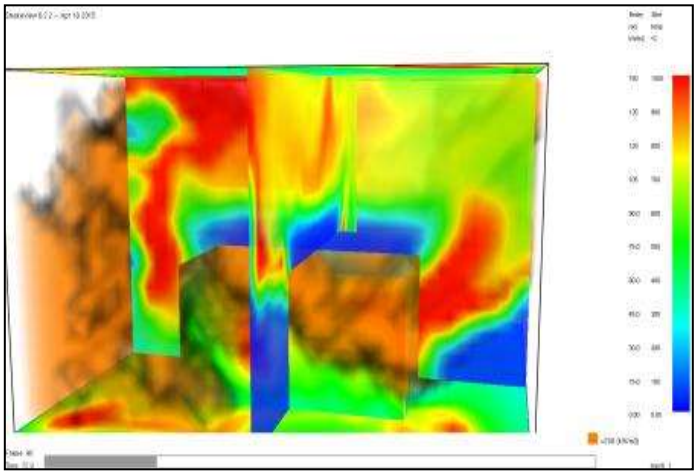

Fig. 8: simulation at frame 40, timestep 72

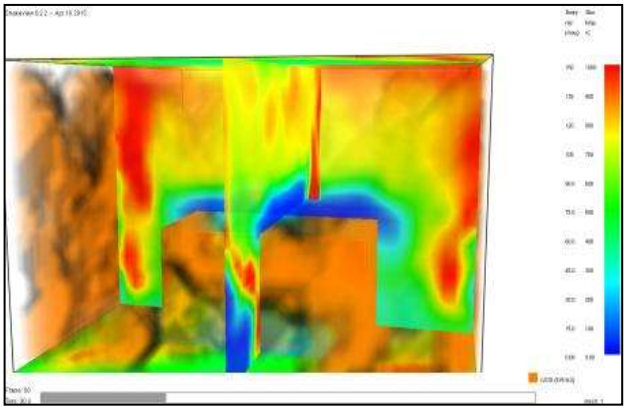

Fig. 9: simulation at frame 50, timestep 90

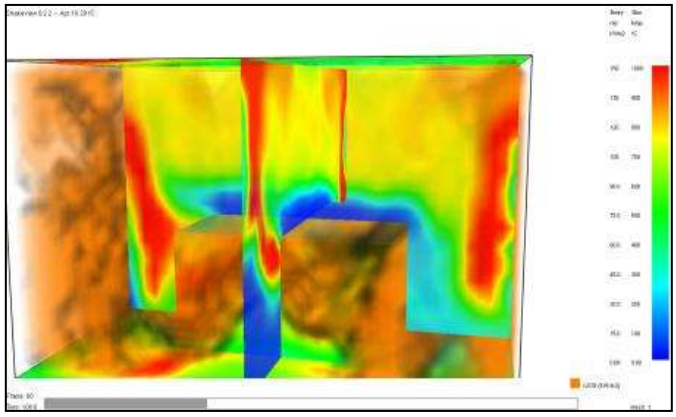

Fig. 10: simulation at frame 60, timestep 10

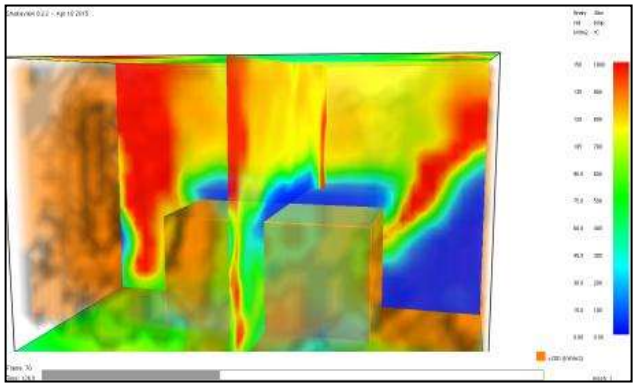

Fig. 11: simulation at frame 70, timestep 126

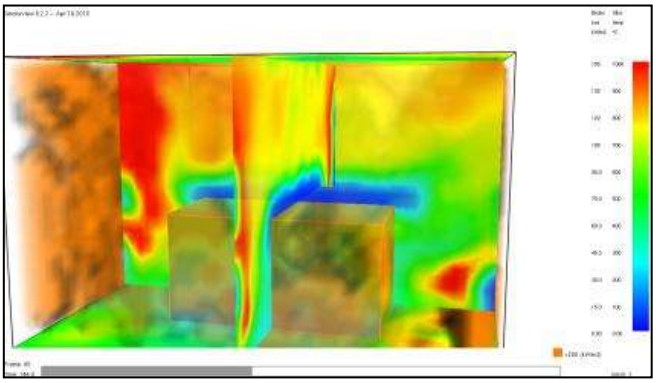

Fig. 12: simulation at frame 80, timestep 144

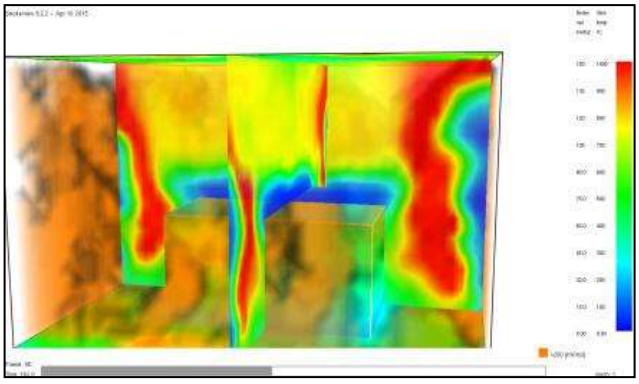

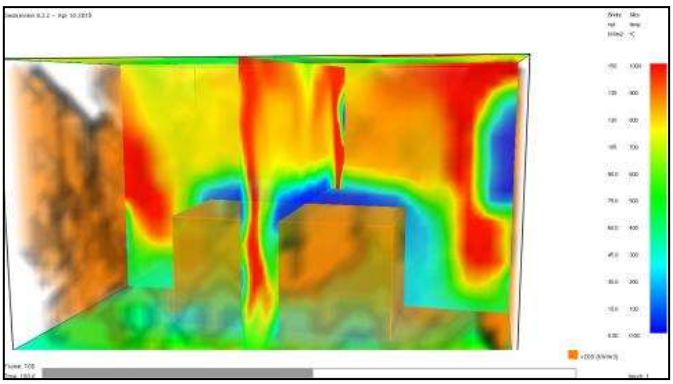

Fig. 13: simulation at frame 90, timestep 162

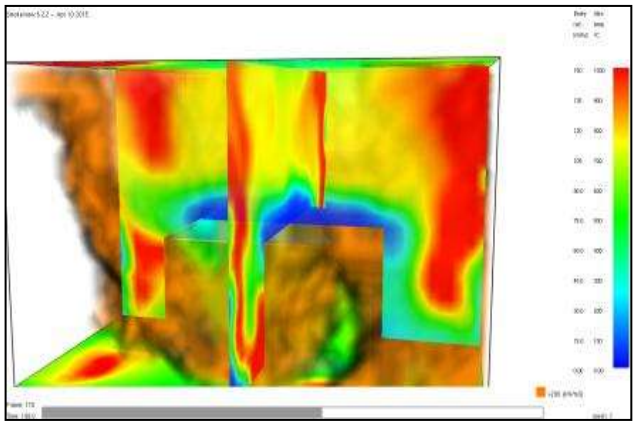

Fig. 14: simulation at frame 100, timestep 180

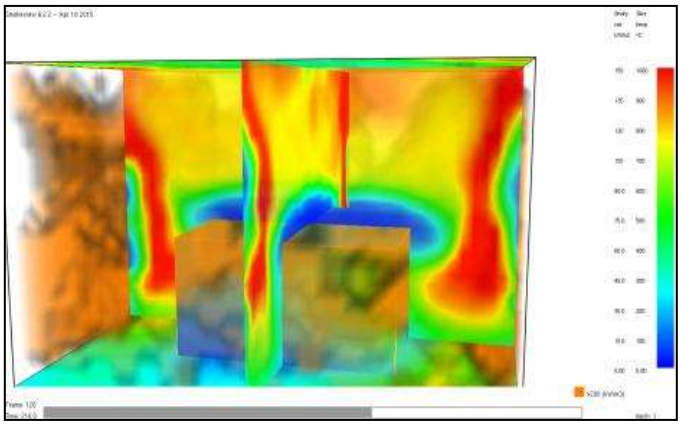

Fig. 15: simulation at frame 110, timestep 198

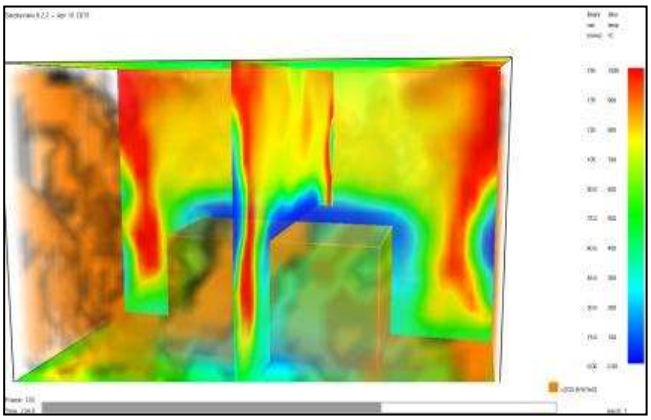

Fig. 16: simulation at frame 120, timestep 216

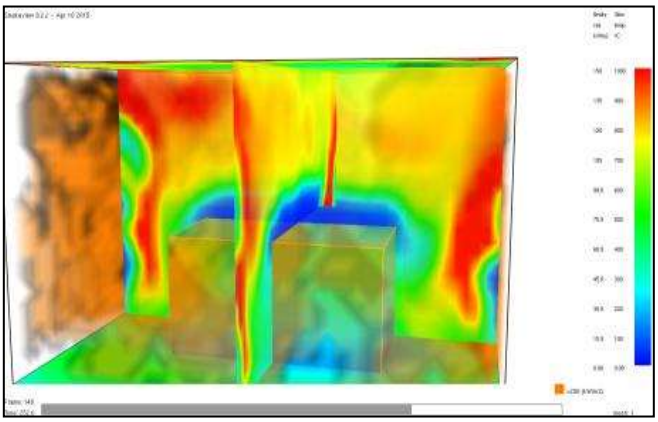

Fig. 17: simulation at frame 130, timestep 234

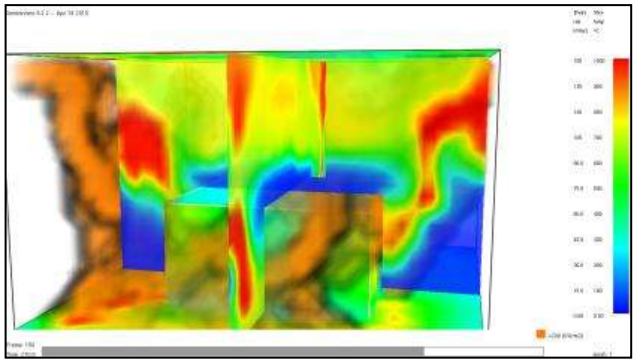

Fig. 18: simulation at frame 140, timestep 252

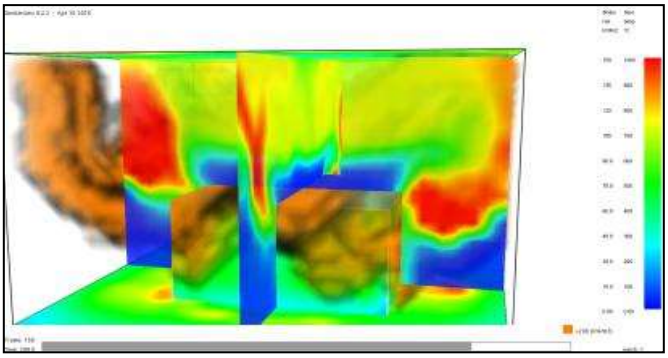

Fig. 19: simulation at frame 150, timestep 270

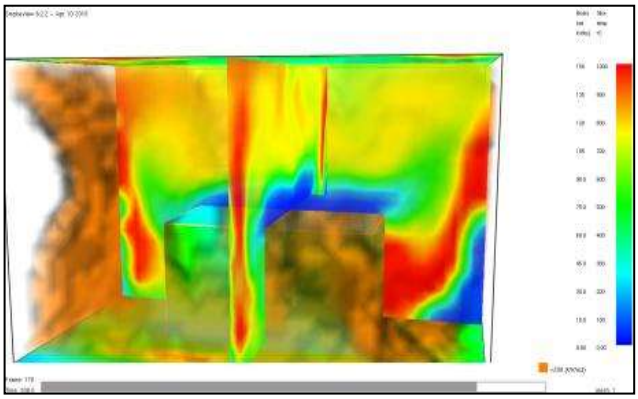

Fig. 20: simulation at frame 180, timestep 288

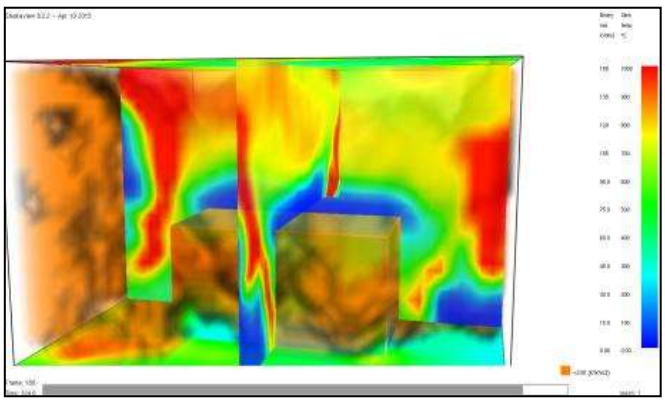

Fig. 21: simulation at frame 150, timestep 270

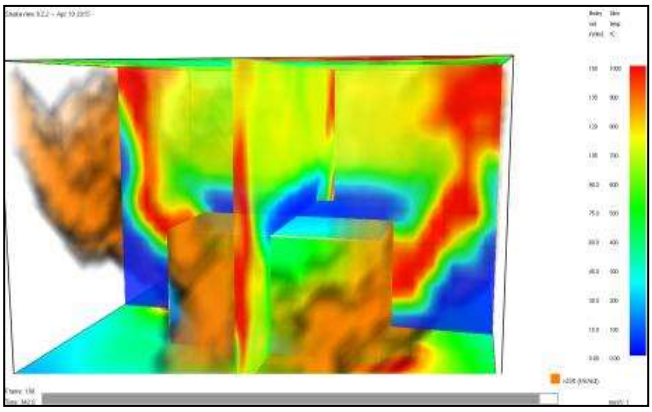

Fig. 22: simulation at frame 180, timestep 288

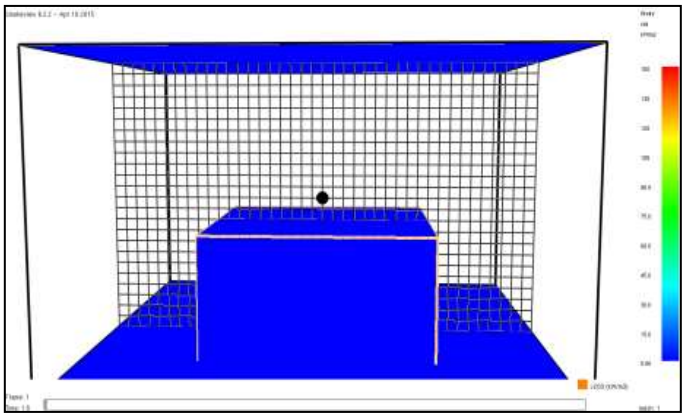

Fig. 23: simulation at frame 190, timestep 342

Fig. 24: simulation at frame 1, timestep 1.8

The simulations as shown b y the rendering which were formed with more than 100,000 grid points and periodic boundary conditions in the mean flow of x. y directions. The periodicity of the combustion of the lumped species causes mixing rates to increase until approximately midway through the simulation. Figures 5, 6 and 7 shows Full Rendering Simulations Showing Combustion, Temperature, Heat Flux and Radiative Heat Characterizations from initial frame and time step of 10 to the final frame and timesteps 324.

Yang et al, 2018 describes these chemical reaction rates are highly nonlinear functions of species concentrations and temperature, which heavily depend on the turbulent mixing. On the other hand, chemical reactions also release heat and subsequently affect species concentrations and temperature, which in turn change the turbulent mixing. Yang et al, 2018 went further asserting that: Chemical reactions occurring at different time scales may interact with eddies of different length/time scales, which further complicates physiochemical processes. The complexities of the turbulence/chemistry interactions as depicted in figures 5, 6 and 7 are considered as the most challenging problem in turbulent combustion modeling.

Figures 5 to 7 shows combustion renderings of temperature, soot, smoke and heat distributions generated from Fire Dynamics Simulator. They are products of computational fluid dynamics (CFD) model of fire-driven fluid flow. These renderings are computer programs, which solves numerically a large eddy simulation form of the Navier–Stokes equations appropriate for low-speed, thermally-driven flow, with an emphasis on smoke and heat transport from fires, to describe the evolution of fire. The column bar to the right of these renderings (figures 5 to 7) depicts the temperature field stratifications/distribution of the combustion/computational space under study. .

In contrast from the renderings (figures 5 to 7) to time-averaged temperature distributions, the instantaneous temperature distributions of the various computational studies, as shown in Figs. 5 to 7, it is observed that irrespective of the computational frame number as well as the computational timestep, the maximum temperature field is 1000^{o}C and the maximum heat release rate per unit area is 150 kW/m^2.

Furthermore, it can be observed, from the renderings (figures 5 to 7), that the modeling of turbulent combustion or combustion is complex as it is complicated and that, to understand its complexities, it is required that we consider the different physico-chemical processes involving a vast range of time and length scales as well as a large number of scalar quantities.

REFERENCES

[1] Bjorn F. Magnussen, The Eddy Dissipation Concept: A Bridge between Science and Technology, ECCOMAS Thematic Conference on Computational Combustion, Lisbon, June 2015
[2] C. K. Westbrook, Y. Mizobuchi, T. J. Poinsot, P. J. Smith, J. Warnatz, Computational Combustion
[3] August 27, 2004, 30th International Symposium on Combustion, Chicago, IL, United States , July 25, 2004 through July 30, 2004
[4] Chin-Hoh Moeng (1984), A large Eddy Simulation Model for the study of Plenary Boundary-layer Turbulence, Journal of Atmospheric Sciences, Vol, 41, No. 13
[5] Curl R.L. (1963) "Dispersed phase mixing: I. Theory and effects in simple reactors", A. I. Ch. E. Journal, 9, 2, 175.
[6] Er. R. K. Rajput (2013), A Textbook book on Fluid Mechanics and Hydraulic Machines in S.I. Units, S. Chand & Company Ltd, Delhi
[7] Gao, X., Zhai, J., Sun, W., Ombrello, T., and Carter, C., "The Effect of Ozone Addition on Autoignition and Flame Stabilization," 54th AIAA Aerospace Sciences Meeting, AIAA Paper 2016-0960, Jan. 2016. doi: 10.2514/6.2016-0960
[8] Gao, X., Sun, W., Ombrello, T., and Carter, C., "The Effect of Ozonolysis Activated Autoignition on Jet Flame Dynamics," 55th AIAA Aerospace Sciences Meeting, AIAA Paper 2017-1776, Jan. 2017. doi: 10.2514/6.2017-1776
[9] Gao, X., Yang, S., Wu, B., and Sun, W., "The effects of ozonolysis activated autoignition on non-premixed jet flame dynamics: a numerical and experimental study," 53rd AIAA/SAE/ASEE Joint Propulsion Conference, Jul. 2017.
[10] Gregory T. Linteris, Lloyd Gewuerz,Kevin McGrattan, and Glenn Forney, Modeling Solid Sample Burning with FDS, Fire Research Division, Building and Fire Research Laboratory, NATIONAL INSTITUTE OF STANDARDS AND TECHNOLOGY, 2004
[11] Hao Wu, Peter C. May, Thomas Jaravelz, and Matthias Ihmex (2017), Application of Pareto-efficient combustion modeling framework to large eddy simulations of turbulent reacting flows, Department of Mechanical Engineering, Stanford University, United States

[12] Huo, H., and Yang, V., "Large-Eddy Simulation of Supercritical Combustion: Model Validation against Gaseous H2-O2 Injector," Journal of Propulsion and Power, 2017. doi: 10.2514/1.B36368
[13] https://www.google.com/url?sa=i&rct=j&q=&esrc=s&source=images&cd=&cad=rja&uact=8&ved=2ahUKEwibu8OElcbeAhUQThoKHWXrDxsQjRx6BAgBEAU&url=https%3A%2F%2Fwww.thoughtco.com%2Fcombustion-reactions-604030&psig=AOvVaw12SPhUB7C19kjzsWcUwT0H&ust=1541813503858510
[14] https://en.wikipedia.org/wiki/Combustion
[15] https://en.wikipedia.org/wiki/Large_eddy_simulation
[16] https://en.wikipedia.org/wiki/Convection%E2%80%93diffusion_equation
[17] J.A. van Oijen *, A. Donini, R.J.M. Bastiaans, J.H.M. ten Thije Boonkkamp, L.P.H. de Goey, State-of-the-art in premixed combustion modeling using flamelet generated manifolds, Progress in Energy and Combustion Science 57 (2016) 30–74
[18] J.W. Deardorff. Stratocumulus-capped mixed layers derived from a three-dimensional model.
[19] Boundary-Layer Meteorol., 18:495–527, 1980. 9
[20] Joan Remski, "The Transport Equation and Directional Derivatives - Introduction," Convergence (August 2004)
[21] Jörgen Carlsson (1999), Fire Modelling Using CFD - An introduction for Fire Safety Engineers, Department of Fire Safety Engineering, Lund Institute of Science and Technology, Lund University.
[22] Kuznetsov V,R" Sabel'nikov V.A. (1990) In Turbulence and Combustion. Hemisphere (Ed.).
[23] New-York.
[24] Michael Stöllinger and Stefan Heinz, PDF Modeling and Simulation of Premixed Turbulent Combustion, Monte Carlo Methods Appl. Vol. No. (), pp. 1–43
[25] P. Ourano, M. Gorokhovskl and R. Borghl, An Application of the Probability Density Function Model to Diesel Engine Combustion, Combust, Sci.and Tech., 1999, Vol. 144, pp.47-78
[26] Pierce, C. D., and Moin, P., "Progress-variable approach for large-eddy simulation of non-premixed turbulent combustion," Journal of Fluid Mechanics, Vol. 504, 2004, pp. 73-97. doi: 10.1017/S0022112004008213
[27] Poinsot T, Veynante D. Theoretical and numerical combustion. 3rd ed. 2011.
[28] R.A. Sweet. Direct Methods for the Solution of Poisson's Equation on a Staggered Grid. Journal of
[29] Computational Physics, 12:422–428, 1973. 9, 37
[30] Williams FA. Combustion theory. Redwood City (CA): Addison-Wesley Publishing Company; 1985.
[31] R.G. Rehm and H.R. Baum. The Equations of Motion for Thermally Driven, Buoyant Flows. Journal
[32] of Research of the NBS, 83:297–308, 1978. 2, 8, 13, 111
[33] Sandia Flame E. In AIAA Aerospace Sciences Meeting (210059 ed.). American Institute of Aeronautics and Astronautics Inc, AIAA. https://doi.org/10.2514/6.2018-1427
[34] Shi, X., Ryu, J. I., Chen, J.-Y., and Dibble, R. W., "Modes of reaction front propagation and end-gas combustion of hydrogen/air mixtures in a closed chamber," International Journal of Hydrogen Energy, Vol. 42, No. 15, 2017, pp. 10501-10512.
[35] Stephen B. Pope. Turbulent Flows. Cambridge University Press, 2000. 9, 23, 25, 26, 27, 32, 46, 85,
[36] 131
[37] T. Echekki, E. Mastorakos (eds.), Turbulent Combustion Modeling, Fluid Mechanics and Its Applications 95 © Springer Science+Business Media B.V. 2011, 439
[38] Yang, S., Wang, X., Yang, V., & Sun, W. (2018). Comparison of finite-rate chemistry and flamelet/progress-variable models II:
[39] Ying Xu, Numerical Modeling and Combustion Studies of Scramjet Problem, A PhD Dissertation, Applied Mathematics and Statistic, Stony Brook University, December 2014.
[40] Zenghua Yan (1999), Numerical Modeling of Turbulent Combustion and Flame Spread, Lund University, Sweden